MATHEMATICAL MODELING AND SIMULATION OF INDUCTION MOTOR WITH EDDY CURRENT LEAKAGE INDUCTANCE IN THE CORE LOSS BRANCH

OLIMPIU STOICUTA[1]

Abstract: The article presents the parallel mathematical model of the induction motor in which the stator iron core losses are modeled taking into account the core loss resistance and the eddy currents leakage inductance, in series connected in the base loss branch of the equivalent circuit of the motor. The induction motor simulation program is made in Matlab-Simulink and is based on the use of an S-Function block.

Keywords: iron core losses, induction machines, eddy currents, simulation.

1. INTRODUCTION

Currently, the vast majority of field-oriented control (FOC) algorithms of induction machines are based on the mathematical model of the machine in which iron losses are neglected [2], [4], [11], [18], [19].

E. Levi, as well as other researchers have shown that these iron losses cannot be neglected when voltage source type inverters (VSI) are used in the vector control systems of induction machines [5] - [9], [12] - [15], [17]. Neglecting the iron losses in the mathematical model of the induction motor leads to reduced dynamic performances of the vector control system [6],[7].

Considering the mentioned, this article presents the parallel mathematical model of the induction motor, in which the losses from the stator iron, as well as the losses due to the eddy currents, are modeled by means of a series RL circuit, placed in parallel with the mutual inductance, in within the equivalent circuit of the induction motor [7]. This type of mathematical model of the induction machine was suggested for the first time by Boldea and Nasar in 1987, and then it was investigated by several researchers [3].

In this context, this article presents in detail how to use the S-Function block, specific to the Matlab-Simulink program [10], [16], in order to modeling and numerical simulation the induction motor in which iron losses are not neglected.

---

[1] *Associate Proffesor Eng. , Ph.D. at the University of Petroşani.*

2. THE PARALLEL MODEL OF THE INDUCTION MOTOR

The equivalent circuit of the induction motor in which iron losses are not neglected, is presented in Fig.1 [7].

In order to model the iron losses in the stator, an RL series connection is used, consisting of the resistance of the stator iron (R_f) and the eddy currents leakage inductance (L_f). In the equivalent circuit of the induction motor, the series RL connection is placed in parallel with the mutual inductance. By means of the leakage inductance (L_f) the rate of change of the eddy currents iron loss is modeled.
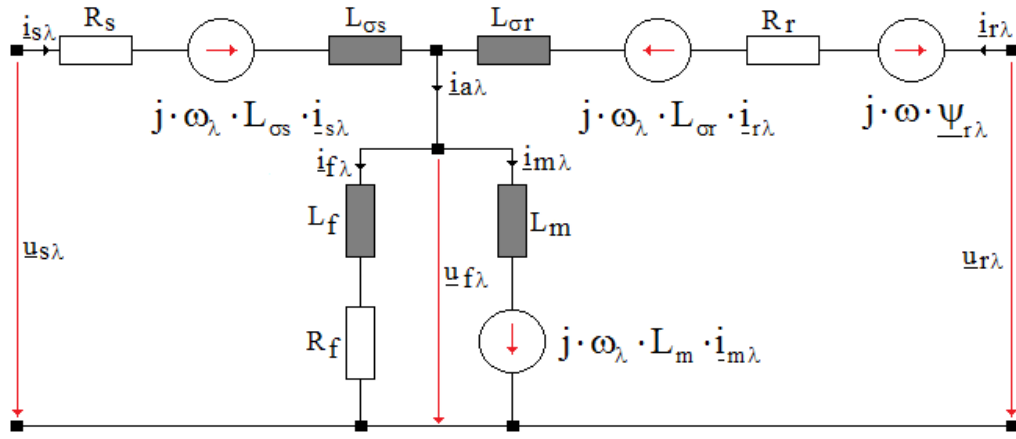

Fig. 1. The equivalent circuit of the induction motor

Based on the equivalent circuit in Fig.1, the equations that define the parallel mathematical model of the induction motor can be determined very easily. The mathematical relationships that can be written based on the circuit in Fig.1, are [7]:

- the stator voltages equation

$$\underline{u}_{s\lambda} = R_s \cdot \underline{i}_{s\lambda} + \frac{d}{dt}\underline{\psi}_{s\lambda} + j \cdot \omega_{\lambda} \cdot \underline{\psi}_{s\lambda} \tag{1}$$

- the rotor voltages equation

$$0 = R_r \cdot \underline{i}_{r\lambda} + \frac{d}{dt}\underline{\psi}_{r\lambda} + j \cdot (\omega_{\lambda} - \omega) \cdot \underline{\psi}_{r\lambda} \tag{2}$$

- the stator flux equation

$$\underline{\psi}_{s\lambda} = \underline{\psi}_{m\lambda} + L_{\sigma s} \cdot \underline{i}_{s\lambda} \tag{3}$$

- the rotor flux equation

$$\underline{\psi}_{r\lambda} = \underline{\psi}_{m\lambda} + L_{\sigma r} \cdot \underline{i}_{r\lambda} \tag{4}$$

- the air-gap flux equation

$$\underline{\psi}_{m\lambda} = L_m \cdot \underline{i}_{m\lambda} \tag{5}$$

- the currents equation

$$\underline{i}_{s\lambda} + \underline{i}_{r\lambda} = \underline{i}_{m\lambda} + \underline{i}_{f\lambda} \tag{6}$$

- magnetic branch voltage equation

$$\underline{u}_{f\lambda} = R_f \cdot \underline{i}_{f\lambda} + L_f \cdot \frac{d}{dt}\underline{i}_{f\lambda} = \frac{d}{dt}\underline{\psi}_{m\lambda} + j \cdot \omega_\lambda \cdot \underline{\psi}_{m\lambda} \tag{7}$$

- motion equation of the induction motor

$$J \cdot \frac{d}{dt}\omega_r = T_e - F \cdot \omega_r - T_L \tag{8}$$

where T_e is the electromagnetic torque and T_L is the load torque

$$T_e = \frac{3}{2} \cdot \frac{z_p}{L_{\sigma r}} \cdot \mathrm{Im}\left(\underline{\psi}_{r\lambda}^* \cdot \underline{\psi}_{m\lambda}\right) \tag{9}$$

The following notations were used in the above relationships:

$$\underline{u}_{s\lambda} = u_{ds\lambda} + j \cdot u_{qs\lambda} \,;\; \underline{u}_{f\lambda} = u_{df\lambda} + j \cdot u_{qf\lambda} \,;\; \underline{i}_{s\lambda} = i_{ds\lambda} + j \cdot i_{qs\lambda} \,;\; \underline{i}_{r\lambda} = i_{dr\lambda} + j \cdot i_{qr\lambda} \,;$$
$$\underline{i}_{m\lambda} = i_{dm\lambda} + j \cdot i_{qm\lambda} \,;\; \underline{i}_{f\lambda} = i_{df\lambda} + j \cdot i_{qf\lambda} \,;\; \underline{\psi}_{s\lambda} = \psi_{ds\lambda} + j \cdot \psi_{qs\lambda} \,;\; \underline{\psi}_{r\lambda} = \psi_{dr\lambda} + j \cdot \psi_{qr\lambda} \,;$$
$$\underline{\psi}_{r\lambda}^* = \psi_{dr\lambda} - j \cdot \psi_{qr\lambda} \,;\; \underline{\psi}_{m\lambda} = \psi_{dm\lambda} + j \cdot \psi_{qm\lambda} \,;\; j = \sqrt{-1} \,;\; \omega = z_p \cdot \omega_r .$$

The previously presented relations are written in an orthogonal reference system $d\lambda - q\lambda$ which rotates with the angular speed $\omega_\lambda = d\lambda/dt$.

The previous relations can be put in matrix form. In the following we will present the *stator currents-rotor fluxes-air-gap fluxes* mathematical model.

$$\frac{d}{dt}\begin{bmatrix} \underline{i}_{s\lambda} \\ \underline{\psi}_{r\lambda} \\ \underline{\psi}_{m\lambda} \end{bmatrix} = \begin{bmatrix} a_{11} & a_{12} & a_{13} \\ 0 & a_{22} & a_{23} \\ a_{31} & a_{32} & a_{33} \end{bmatrix} \cdot \begin{bmatrix} \underline{i}_{s\lambda} \\ \underline{\psi}_{r\lambda} \\ \underline{\psi}_{m\lambda} \end{bmatrix} + \begin{bmatrix} b_{11} \\ 0 \\ b_{31} \end{bmatrix} \cdot \underline{u}_{s\lambda} \tag{10}$$

$$\frac{d}{dt}\omega_r = H_{m1} \cdot \text{Im}\left(\underline{\psi}_{r\lambda}^* \cdot \underline{\psi}_{m\lambda}\right) - H_{m2} \cdot \omega_r - H_{m3} \cdot T_L \tag{11}$$

where $\sigma_a = \dfrac{L_{\sigma s} \cdot k_1}{L_{\sigma s} \cdot k_1 - 1}$; $k_1 = k_{1a} + k_{1b}$; $k_{1a} = \dfrac{1}{L_f} + \dfrac{1}{L_{\sigma s}}$; $k_{1b} = \dfrac{1}{L_{\sigma r}} + \dfrac{1}{L_m}$; $\gamma = \dfrac{1}{\sigma_a}$;

$a_{11} = a_{11\_re} + a_{11\_im} \cdot j \cdot \omega_\lambda$; $a_{11\_re} = -\gamma \cdot \left(\dfrac{1}{T_{\sigma s}} + \dfrac{1-\gamma}{\gamma \cdot T_f}\right)$; $a_{11\_im} = -\gamma$; $T_{\sigma s} = \dfrac{L_{\sigma s}}{R_s}$; $T_f = \dfrac{L_f}{R_f}$;

$a_{12} = a_{12\_re} + a_{12\_im} \cdot j \cdot (\omega_\lambda - \omega)$; $a_{12\_re} = \dfrac{\gamma-1}{L_{\sigma r}} \cdot \left(\dfrac{1}{T_f} - \dfrac{1}{T_{\sigma r}}\right)$; $a_{12\_im} = \dfrac{1-\gamma}{L_{\sigma r}}$; $T_{\sigma r} = \dfrac{L_{\sigma r}}{R_r}$;

$a_{13} = a_{13\_re} + a_{13\_im} \cdot j \cdot \omega_\lambda$; $a_{13\_re} = (\gamma-1) \cdot \left(\dfrac{1}{T_{\sigma r} \cdot L_{\sigma r}} - \dfrac{k_{1b}}{T_f}\right)$; $a_{13\_im} = (\gamma-1) \cdot k_{1b}$;

$a_{22} = a_{22\_re} - j \cdot (\omega_\lambda - \omega)$; $a_{23} = -a_{22\_re}$; $a_{22\_re} = -\dfrac{1}{T_{\sigma r}}$; $b_{11} = \dfrac{\gamma}{L_{\sigma s}}$; $\omega = z_p \cdot \omega_r$;

$a_{31} = a_{31\_re} + a_{31\_im} \cdot j \cdot \omega_\lambda$; $a_{31\_re} = L_{\sigma s} \cdot (1-\gamma) \cdot \left(\dfrac{1}{T_f} - \dfrac{1}{T_{\sigma s}}\right)$; $a_{31\_im} = L_{\sigma s} \cdot (\gamma-1)$;

$a_{32} = a_{32\_re} + a_{32\_im} \cdot j \cdot (\omega_\lambda - \omega)$; $a_{32\_re} = -L_{\sigma s} \cdot a_{12\_re}$; $a_{32\_im} = -L_{\sigma s} \cdot a_{12\_im}$;

$a_{33} = a_{33\_re} + a_{33\_im} \cdot j \cdot \omega_\lambda$; $a_{33\_re} = -L_{\sigma s} \cdot a_{13\_re}$; $a_{33\_im} = L_{\sigma s} \cdot (\gamma-1) \cdot k_{1a}$; $b_{31} = 1-\gamma$;

$H_{m1} = \dfrac{3}{2} \cdot \dfrac{z_p}{J} \cdot \dfrac{1}{L_{\sigma r}}$; $H_{m2} = \dfrac{F}{J}$; $H_{m3} = \dfrac{1}{J}$; $L_r = L_{\sigma r} + L_m$; $L_s = L_{\sigma s} + L_m$; $j = \sqrt{-1}$.

When $\omega_\lambda = 0$ in (10), we obtain the mathematical model in stator reference of the induction motor. On the other hand, the mathematical model of the induction motor in rotor reference, is obtained when in relation (10) we have $\omega_\lambda = \omega$.

3. NUMERICAL SIMULATION OF THE INDUCTION MOTOR

The mathematical model of the induction motor, which is simulated in Matlab-Simulink based on an S-Function type block, is given by relations (10) and (11), for $\omega_\lambda = 0$. In the simulation, starting the induction motor is of the direct on-line (DOL) type, in load (the load torque is equal to the rated torque).

In order to numerical simulate, a 1.5 [kW] induction motor is used, which has the electrical and mechanical parameters given in table 1.

*Table 1. **The electrical and mechanical parameters of the induction motor [1]***

	Name	Value		Name	Value
R_s	*Stator resistance*	4.85 [Ω]	J	*Motor inertia*	0.031[kg·m^2]
R_r	*Rotor resistance*	3.805 [Ω]	F	*Friction coefficient*	0.008[N·m·s/rad]

R_f	Core loss resistance	500 [Ω]	n_N	Rated speed	1420 [rpm]
L_s	Stator inductance	0.274 [H]	z_p	Number of pole pairs	2
L_r	Rotor inductance	0.274 [H]	f_N	Rated frequency	50 [Hz]
L_m	Mutual inductance	0.258 [H]	U_N	Rated voltage	220 Δ/380 Y [V]
L_f	Eddy currents leakage inductance	0.1 [H]	M_N	Rated torque	10 [N·m]

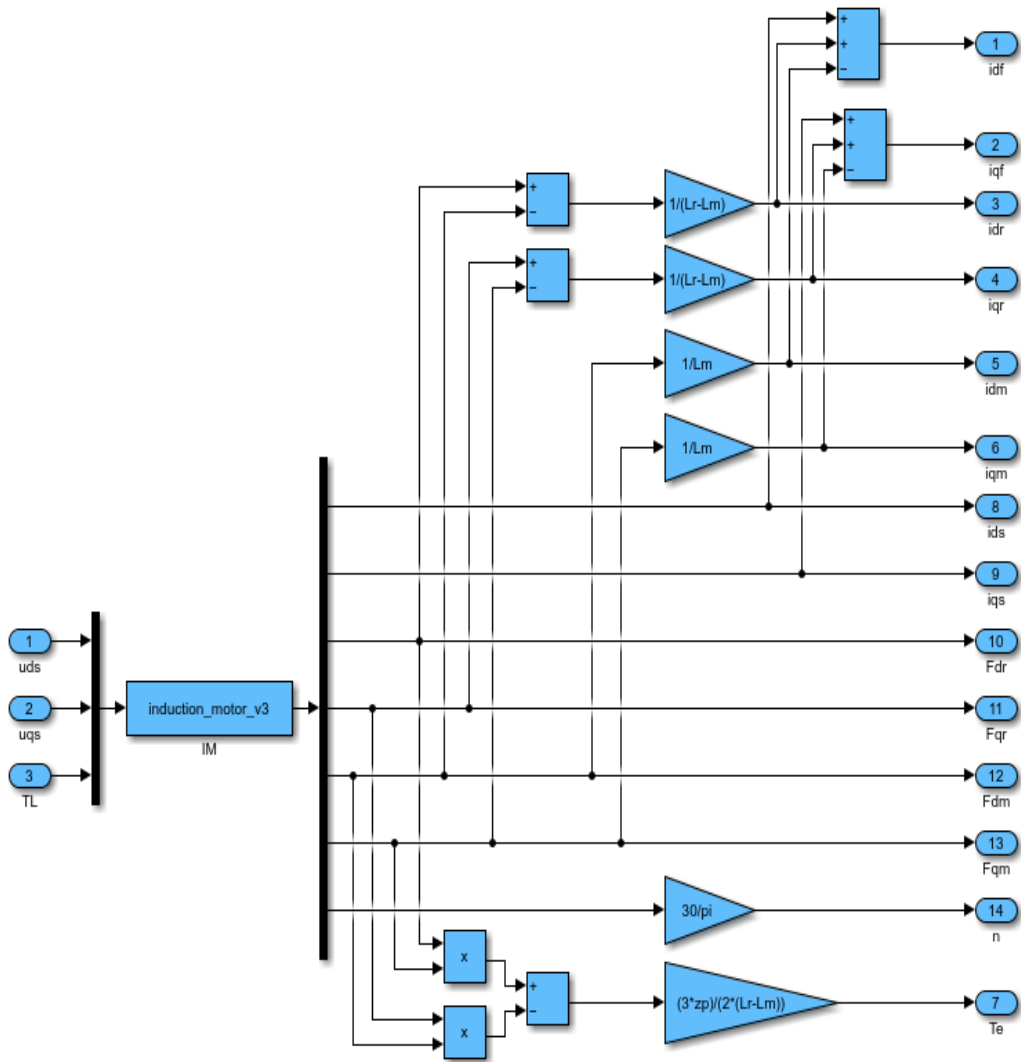The induction motor simulation program is presented in Fig. 2.
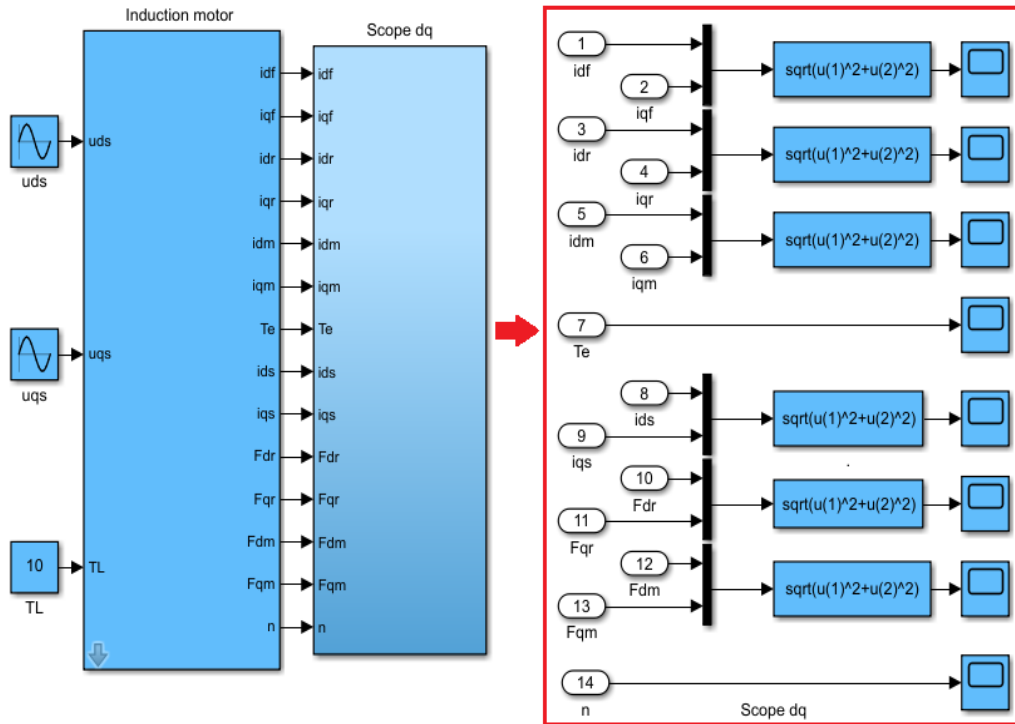
Fig. 2. The induction motor simulation program

The internal structure of the "Induction motor" block (from Fig.2), is presented in Fig.3.

Within the simulation program, the d-q components of the stator voltages are given by the following relations

$$\begin{cases} u_{ds} = U_N \cdot \sqrt{\dfrac{2}{3}} \cdot \sin(\omega \cdot t) \\ u_{qs} = U_N \cdot \sqrt{\dfrac{2}{3}} \cdot \sin\left(\omega \cdot t - \dfrac{\pi}{2}\right) \end{cases} \qquad (12)$$

where: $U_N = 380 [V]$; $\omega = 2 \cdot \pi \cdot f$; $f = 50 [Hz]$.

Fig. 3. The internal structure of the "Induction motor" block

In Fig.3, the "IM" block is of the S-Function type. The Matlab program attached to this block is shown in Fig.4.

The parameters of the S-Function block (from Fig.3) are: Rs, Rr, Rf, Lf, Ls, Lr, Lm, J, F, zp (see Table 1). The "Induction motor" block (see Fig. 2) is obtained based on the program shown in Fig. 3, using the operation of creating a subsystem (shortcut key: Ctrl+G), specific to the Simulink program. On the other hand, the "Induction motor" block (from Fig.2) has a created mask (shortcut key: Ctrl+M), in which electrical and mechanical parameters of the induction motor are entered (see Table 1).

```matlab
function [sys,x0]=induction_motor_v3(t,x,u,flag,Rs,Rr,Rf,Lf,Ls,Lr,Lm,J,F,zp)
Lgs=Ls-Lm;
Lgr=Lr-Lm;
Tgs=Lgs/Rs;
Tgr=Lgr/Rr;
Tf=Lf/Rf;
k1a=(1/Lf) +(1/Lgs);
k1b=(1/Lgr) +(1/Lm);
k1=k1a+k1b;
ga=(Lgs*k1)/(Lgs*k1-1);
gam=1/ga;
a11_re=-gam*((1/Tgs) +(1-gam)/(gam*Tf));
a12_re=((gam-1)/Lgr) *((1/Tf) -(1/Tgr));
a12_im=(1-gam)/Lgr;
a13_re=(gam-1) *((1/(Tgr*Lgr))-k1b/Tf);
a22_re=-1/Tgr;
a31_re=Lgs*(1-gam) *((1/Tf) -(1/Tgs));
a32_re=-Lgs*a12_re;
a32_im=-Lgs*a12_im;
a33_re=-Lgs*a13_re;
b11=gam/Lgs;
b31=1-gam;
Hm1=(3*zp)/(2*J*Lgr);
Hm2=F/J;
Hm3=1/J;
if abs(flag)==1
    sys=[a11_re*x(1)+a12_re*x(3)+a12_im*zp*x(7)*x(4)+a13_re*x(5)+b11*u(1);
         a11_re*x(2)+a12_re*x(4)-a12_im*zp*x(7)*x(3)+a13_re*x(6)+b11*u(2);
         a22_re*x(3)-zp*x(7)*x(4)-a22_re*x(5);
         a22_re*x(4)+zp*x(7)*x(3)-a22_re*x(6);
         a31_re*x(1)+a32_re*x(3)+a32_im*zp*x(7)*x(4)+a33_re*x(5)+b31*u(1);
         a31_re*x(2)+a32_re*x(4)-a32_im*zp*x(7)*x(3)+a33_re*x(6)+b31*u(2);
         Hm1*x(3)*x(6)-Hm1*x(4)*x(5)-Hm2*x(7)-Hm3*u(3)];
elseif flag==3
   sys=x;
elseif flag==0
   sys=[7 0 7 3 0 0];
    x0=[0;0;0;0;0;0];
else
   sys=[];
end
```

Fig. 4. The Matlab program of the "IM" block

The simulation of the induction motor is done using the Dormand-Prince numerical method (ode45), which has a relative and absolute error of $\varepsilon = 10^{-7}$.

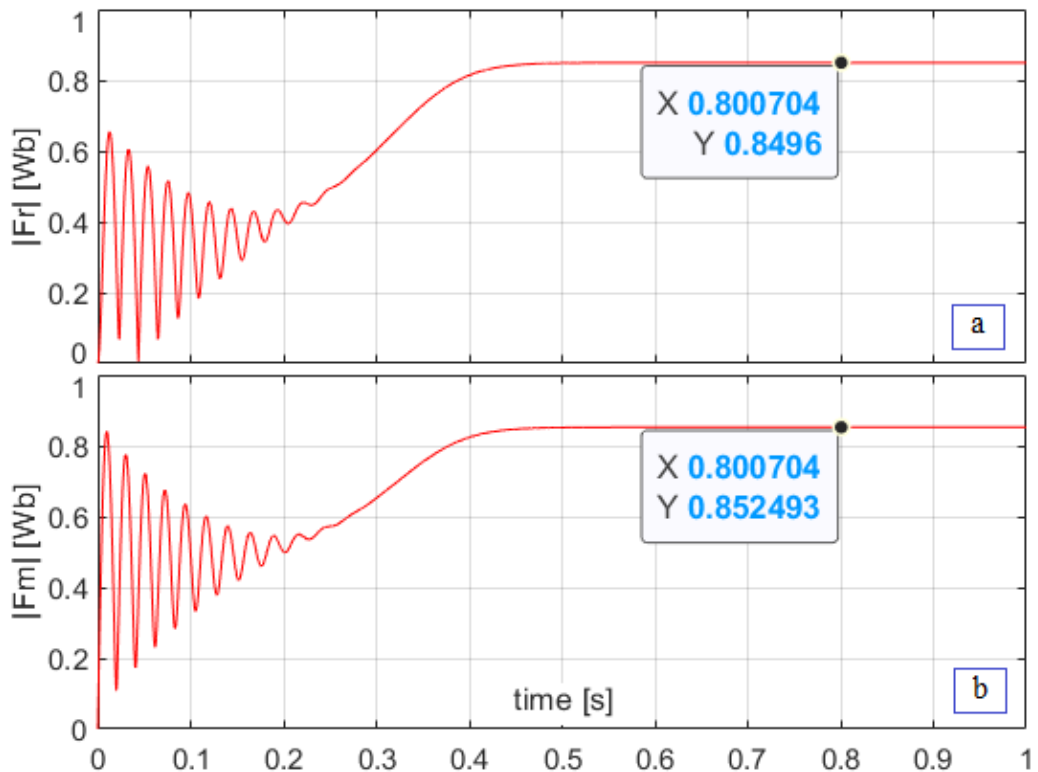The results obtained after the simulation are presented in the following figures

123

Fig. 5. The rotor flux (a) and the air-gap flux (b) space vectors - absolute values
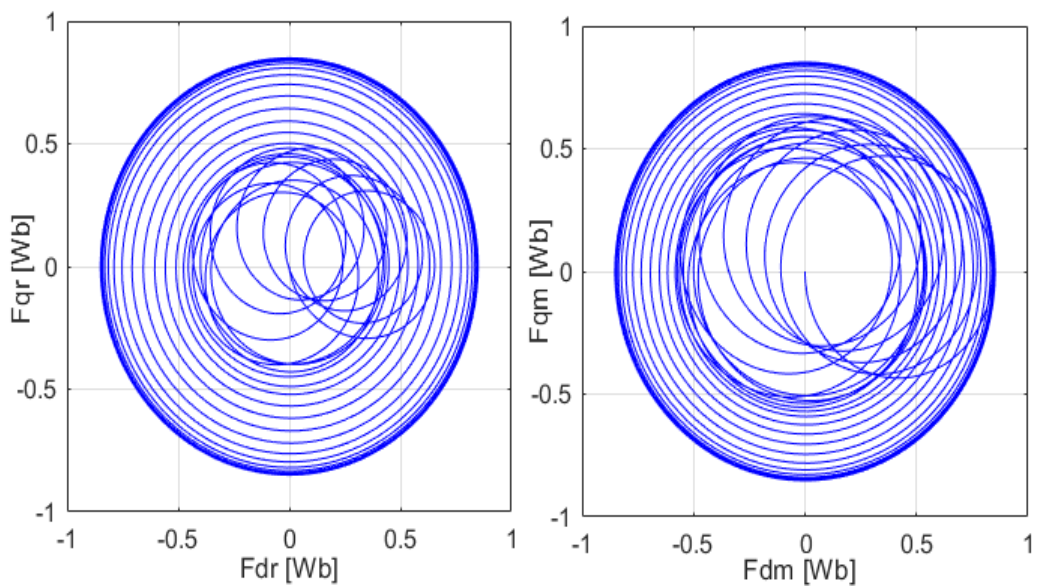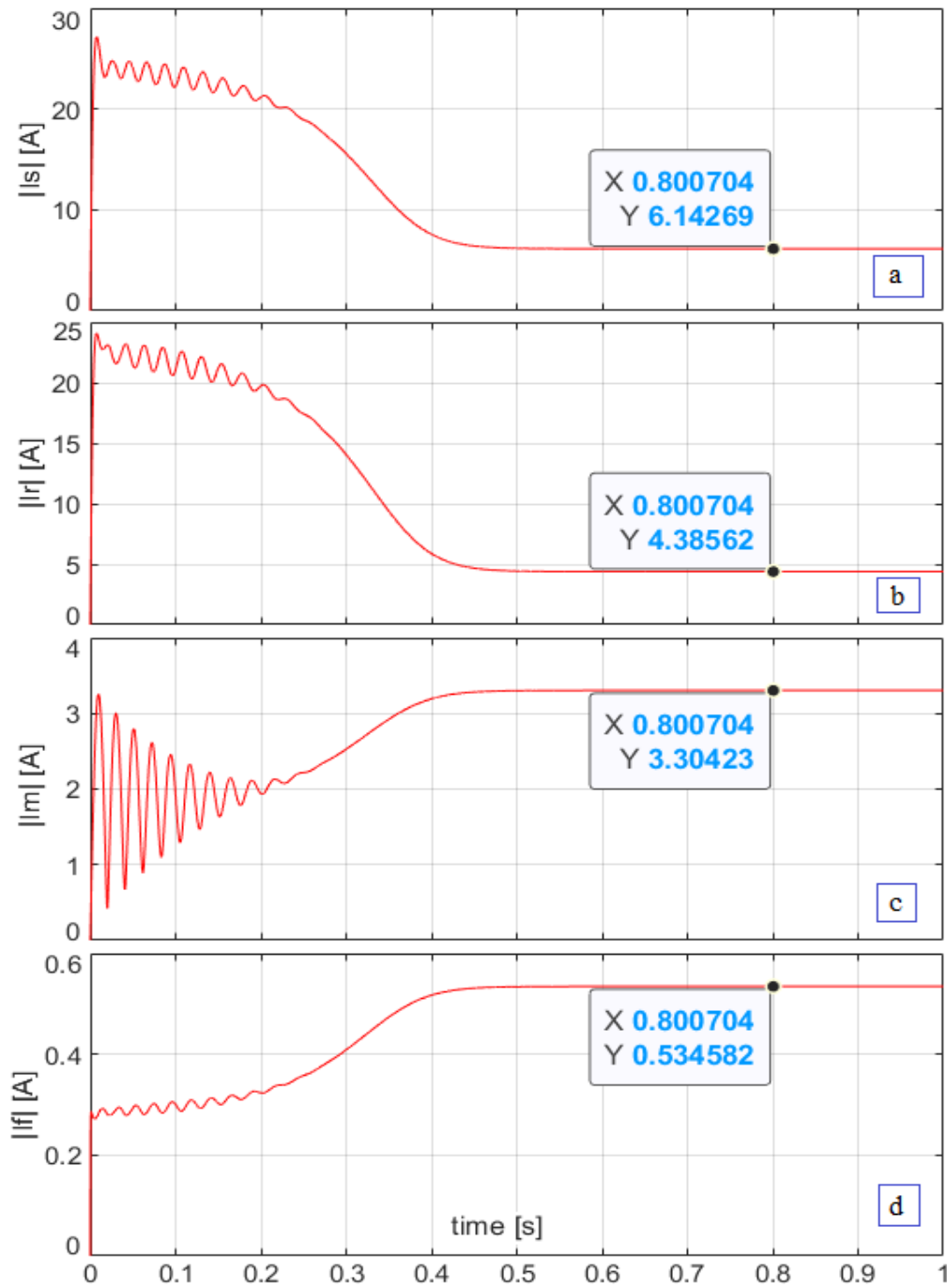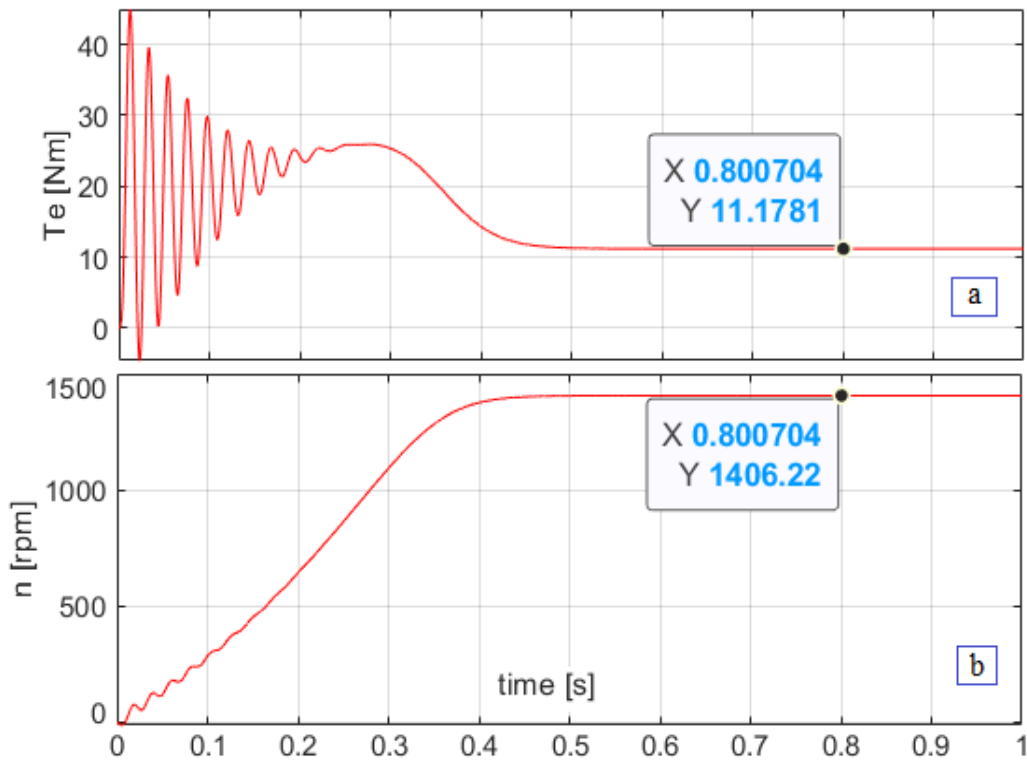

Fig. 6. The trajectory of the rotor flux (a) and of the air-gap flux (b) - space vectors

Fig. 7. The currents space vectors - absolute values
(a) the stator current; (b) the rotor current; (c) the magnetizing current; (d) the current
through the core loss branch

Fig. 8. The electromagnetic torque (a) - The speed of the induction motor (b)

From Fig.8 it can be seen that the induction motor, upon direct application of the supply voltages, starts the load without problems, reaching a speed of 1406 [rpm], after a time of 0.5 [s]. At the same time, the electromagnetic torque developed by the induction motor reaches the approximate value of 11 [Nm].

On the other hand, from Fig.7, it can be seen that both in transient mode and in stationary mode, we can write the following inequalities between the values of the induction motor currents space vectors: $\left|\underline{i}_s\right| > \left|\underline{i}_r\right| > \left|\underline{i}_m\right| > \left|\underline{i}_f\right|$.

At the moment of starting in load of the induction motor, the module of the stator current space vector reaches the value of 27.13 [A], while the module of the rotor current space vector reaches the value of 24. 08 [A]. The time at which these maximum values are reached is approximately 7.5 [ms].

The trajectories of the space vectors of the rotor flux and of the air-gap flux are perfectly circular in stationary regime (see Fig. 6). Due to the direct start in the load, the trajectories of the two space vectors, in transitory regime, show oscillations that amortize in time (see Fig. 6). These oscillations stabilize after a time of approximately 0.5 [s] (see Fig.5).

On the other hand, from Fig. 5, it can be seen that: $\left|\underline{\psi}_m\right| > \left|\underline{\psi}_r\right|$ (this inequality is valid both in transitory regime and in stationary regime).

4. CONCLUSIONS

The inclusion of the eddy current leakage inductance in the core loss branch complicates the parallel mathematical model of the induction motor. The number of mathematical operations increases, and the 3x1 vector that multiplies the stator voltage space vector, has an additional element, compared to the mathematical model in which the eddy current leakage inductance is not taken into account. On the other hand, the inclusion of the eddy current leakage inductance in the core loss branch does not significantly increase the accuracy of the mathematical model of the induction motor. However, the use of the mathematical model presented in this article in the vector control systems of the speed of induction motors can lead to better dynamic performances, in terms of the dynamics of flux and/or speed observers.

The detailed presentation of both the mathematical model and the induction motor simulation program offers specialists a very useful support. The induction motor simulation program is based on the use of an S-Function type block, specific to the Simulink program.

REFERENCES

[1].**Aissa K., Eddine K.D.,** *Vector control using Series Iron Loss Model of Induction Motors and Power Loss Minimization,* World Academy of Science, Engineering and Technology, Vol.52, pp. 142-148, 2009.

[2].**Boldea I., Nasar S.A.,** *Vector Control of AC Drives,* CRC Press, 1992.

[3].**Boldea I., Nasar S.A.,** *Unified Treatment of Core Losses and Saturation in the Orthogonal-Axis Model of Electric Machines,* IEE Proceedings B, Electric Power Applications, Vol.134, No. 6, pp.355-363, 1987.

[4].**Kelemen A., Imecs M.,** *Field-oriented AC Electrical Drives*, Romania Academy Publishing House, Bucharest, 1989.

[5].**Kubota K., Matsuse K.,** *Compensation for core loss of adaptive flux observer-based field-oriented induction motor drives*, Proceedings of the 1992 International Conference on Industrial Electronics, Control, Instrumentation, and Automation, vol.1, pp. 67-71, 1992.

[6].**Levi E.,** *Impact of Iron Loss on Behavior of Vector Controlled Induction Machines,* IEEE Transactions on Industry Applications, vol.31, pp.1287-1296, 1995.

[7].**Levi E.,** *Iron core loss effects in indirect rotor flux oriented induction machines*, Proceedings of Melecon'94, Mediterranean Electrotechnical Conference, Vol.2, pp. 766-769, 1994.

[8].**Levi E., Sokola M., Boglietti A., Pastorelli M.,** *Iron loss in rotor-flux-oriented induction machines: identification, assessment of detuning, and compensation*, in IEEE Transactions on Power Electronics, Vol. 11, no. 5, pp. 698-709, 1996.

[9].**Nasir B.A,** *An Accurate Iron Core Loss Model in Equivalent Circuit of Induction Machines*, Journal of Energy, vol. 2020, pp. 1-10, 2020.

[10]. **Ong C.H.,** *Dynamic Simulations of Electric Machinery: using Matlab-Simulink*, Prentice Hall, 1998.

[11]. **Pana T., Stoicuta O.,** *Stability of the Vector Drive Systems with Induction Motors,* Mediamira Publishers, 2016.

[12]. **Rasmussen H., Vadstrup P., Borsting H.,** *Rotor field oriented control with adaptive iron loss compensation*, Conference Record of the 1999 IEEE Industry Applications Conference. Thirty-Forth IAS Annual Meeting, vol.2, pp. 1253-1258, 1999.

[13]. Sokola M., Levi E., *Combined impact of iron loss and main flux saturation on operation of vector controlled induction machines*, 1996 6-th International Conference on Power Electronics and Variable Speed Drives Conf., pp. 36-41, 1996.

[14]. Sokola M., Levi E., Jamieson G., Williams D., *Representation and compensation of iron loss in rotor flux oriented induction machines*, Proceedings of International Conference on Power Electronics, Drives and Energy Systems for Industrial Growth, vol.1, pp. 243-249, 1996.

[15]. Stoicuta O., *The utilization of the S-Function block in simulation of the Luenberger rotor flux observer for induction motors*, Annals of the University of Petrosani, Electrical Engineering, Vol.18, pp. 31- 46, 2016.

[16]. Stoicuta O., *The utilization of the S-Function block in simulation of the mathematical model of induction motor with iron loss*, Annals of the University of Petrosani, Electrical Engineering, Vol.18, pp. 5-20, 2016.

[17]. Wang, K., Huai, R., Yu, Z., Zhang, X., Li, F., Zhang, L., *Comparison Study of Induction Motor Models Considering Iron Loss for Electric Drives*, Energies, 12, 503, 2019.

[18]. Werner L., *Control of Electrical Drives*, 3rd edition, Springer 2001.

[19]. Vas P., *Vector Control of AC Machines*, CRC Oxford, 1990.